assessed by flow cytometry. Meniscus cells were co-cultured with progenitor cells in a 20:80 ratio in the absence of growth factors (n=2 donors, 3 pellets per donor). Glycosaminoglycan and DNA content was determined using a dimethylmethylene-Blue (DMMB) and PicoGreen assay.
Results: All progenitor and non-selected meniscus donors demonstrated osteogenic and adipogenic differentiation. All meniscus progenitors showed glycosaminoglycan deposition, indicating chondrogenic differentiation. In none of the of non-selected meniscus cells glycosaminoglycans could be detected by Safranin O staining (figure 1). Of the progenitor cells, 73-87% expressed the surface marker profile according to the ISCT MSC criteria(figure 2). Co-culture of meniscus cells with progenitor cells increased glycosaminoglycan deposition (figure 3).
Conclusions: Meniscus progenitor cells are present in the osteoarthritic human meniscus. In our experimental set-up, meniscus progenitor cells have trilineage potential with higher chondrogenic capacity than the total meniscus cell population. Flow cytometry indicates that meniscus progenitor cells express MSC markers. Due to the high chondrogenic potential, easy isolation and fast proliferation, meniscus progenitor cells are a promising cell source for regeneration of meniscus tissue.

304
MACROSCOPIC AND HISTOLOGIC IMPROVEMENTS IN JOINT CARTILAGE, SUBCHONDRAL BONE AND SYNOVIAL MEMBRANE WITH GLYCOSAMINOGLYCANS AND NATIVE TYPE II COLLAGEN IN A RABBIT MODEL OF OSTEOARTHRITIS

V. Sifre [1], C. Soler [2], J.I. Redondo [3], L. Domenech [3], S. Segarra [4], C.I. Serra [5]. [1] *Escuela de Doctorado. Programa de Ciencias de la Vida y la Naturaleza. Univ. Católica de Valencia, Valencia, Spain;* [2] *Hosp. Veterinario UCV. Univ. Católica de Valencia, Valencia, Spain;* [3] *Univ. CEU Cardenal Herrera, Valencia, Spain;* [4] *Animal Hlth., Bioibérica S.A.U., Barcelona, Spain;* [5] *Departamento de Med. y Cirugía Animal. Univ. Católica de Valencia, Valencia, Spain*

Purpose: To evaluate the effects of an oral combination of chondroitin sulfate (CS), glucosamine hydrochloride (Gl) and hyaluronic acid (HA), with or without native type II collagen (NC), on articular cartilage, subchondral bone and synovial membrane in an experimental model of osteoarthritis induced by anterior cruciate ligament section in rabbits.
Methods: This was a prospective, randomized, double-blinded experimental study. The study protocol was approved by an ethics committee in accordance with article 31 of RD53/2013. Fifty-four 10 weeks old female New Zealand white rabbits were distributed into 3 groups and received a daily oral administration of the following treatments: Group 0 (Control group - no treatment), Group 1 [CS (CS Bioactive®) + Gl + HA (Mobilee®)], and Group 2 [(CS + Gl + HA + NC (b-2Cool®)]. All active ingredients were provided by Bioiberica SAU, Barcelona, Spain. In each group, subjects were divided into 3 subgroups (n=6) based on survival times (28, 56 and 84 days). After quarantine period, section of the anterior cruciate ligament of the right stifle was performed in all rabbits under general anesthesia (intramuscular premedication: medetomidine 50μg/kg, fentanyl 10μg/kg, ketamine 5mg/kg and midazolam 0.5mg/kg; intravenous induction: propofol 2mg/kg; inhalatory maintenance: sevofluorane 2.6% and intravenous enrofloxacin 0.5mg/kg; intraoperative analgesia: fentanyl bolus 2μg/kg and CRI 1μg/kg/h; intravenous recovery: ranitidine 2mg/kg, metoclopramide 0.5mg/kg and meloxicam 0.4mg/kg). Afterwards, animals were kept under controlled conditions of temperature, humidity and photoperiod until sacrifice. After sacrifice, samples of lateral femoral condyle and synovial membrane were obtained. Macroscopic evaluation was performed following a cartilage surface scoring system described by Laverty et al. in 2010, and an osteophytosis staging semiquantitative scale described by Tsuromoto et al. in 2013. For histologic evaluation, and before observation under microscope, samples were fixed with 10% buffered formalin, decalcified and embedded in paraffine blocks to obtain longitudinal sections of 5 microns. Cartilage and subchondral bone sections from the femoral condyle were stained with hematoxylin-eosin and Masson trichrome stain, while synovial membrane sections were stained with hematoxylin-eosin. The OARSI semi-quantitative scale described by Laverty et al. in 2010 was used to evaluate matrix staining, cartilage structure, chondrocyte density and cluster formation. Changes in subchondral bone structure and synovial membrane cellular disposition were assessed by the semiquantitative scales described by Gerwin et al. in 2010. For the statistical analysis, a generalized lineal model has been used, with a statistical significance p-value of <0.05.
Results: As expected when using this model, all rabbits developed degenerative changes associated with osteoarthritis after anterior cruciate ligament section.When groups were compared, and overtime, macroscopic evaluation showed significantly lower values in Group 2, compared to groups 0 and 1, meaning that cartilage appearance in these rabbits was closer to that of a healthy one (Figure 1). Microscopically, the assessment of articular cartilage revealed significantly better results for groups 1 and 2, compared to Control, for matrix staining, cartilage structure, chondrocyte density and synovial membrane, indicating that these groups did not show the degree of degenerative changes observed in the Control group. Regarding microscopical evaluation of the subchondral bone, significantly better results were also seen in groups 1 and 2, compared to Control. On the other hand, histologic evaluation of the synovial membrane showed significantly lower values for Group 2, compared to groups 1 and 0; and significantly lower values for Group 1, compared to Group 0. Overall, the group in which joint structures showed values closer to those of a healthy joint was Group 2, followed by Group 1, and lastly by group 0, which featured a more severe degenerative process of osteoarthritis.
Conclusions: In a rabbit model of induced osteoarthritis, a beneficial treatment effect on articular cartilage, subchondral bone and synovial membrane was achieved following oral administration of the combinations CS+Gl+HA and CS+Gl+HA+NC. Moreover, the addition of NC to CS+Gl+HA allowed the combination CS+Gl+HA+NC to provide even significantly better results in terms of macroscopic cartilage evaluation and microscopic synovial membrane assessment. Although extrapolations between species should be made with caution, data presented herein supports the potential usefulness of these combinations in human and veterinary medicine for the multimodal management of patients with joint conditions.

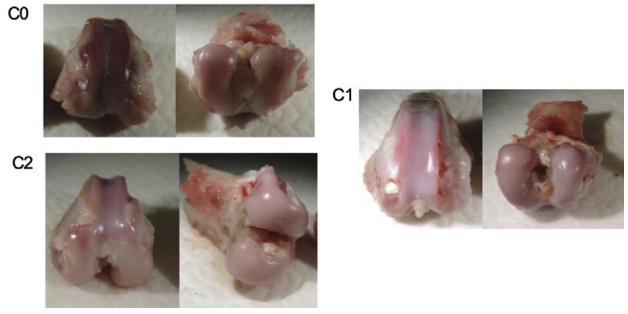

305
ARTICULAR CARTILAGE RESPONSE TO BLUNT VS SHARP LESIONS IN AN IN VIVO EQUINE CARPAL GROOVE MODEL

N. te Moller [1], A. Mohammadi [2], S. Plomp [1], M. Beukers [1], B. Pouran [3], J. Mäkelä [2], R. Korhonen [2], T. Juha [4], H. Brommer [1], R. van Weeren [1]. [1] *Utrecht Univ., Utrecht, Netherlands;* [2] *Univ. of Eastern Finland, Kuopio, Finland;* [3] *Univ. Med. Ctr. Utrecht, Utrecht, Netherlands;* [4] *Univ. of Queensland, Brisbane, Australia*

Purpose: Chondral defects are common in humans and horses and may initiate the development of osteoarthritis. However, if, when and how they should be approached therapeutically is still subject of discussion. In the equine carpal joint, critical size of chondral lesions has been determined at 2mm diameter, beyond which no spontaneous healing occurs. However, the progression of degeneration is likely determined by other factors besides the size of a lesion. In bovine cartilage explants, sharp and blunt trauma lead to different responses in the tissue adjacent to the lesion. A better understanding of the progression of various forms of chondral lesions could help in determining the best (time of) intervention. Therefore, we investigated the long-term response of articular cartilage to artificially created blunt and sharp grooves in the equine carpal joint. We hypothesized that disruption of the collagen network of articular cartilage, combined with intensified loading would always lead to progressive degeneration, but that the presence of initial tissue loss (blunt grooves) would substantially accelerate this process.
Methods: In one randomly assigned front limb of nine adult female Shetland ponies the cartilage layers at the proximal surface of the intermediate carpal bone and at the radial facet of the third carpal bone

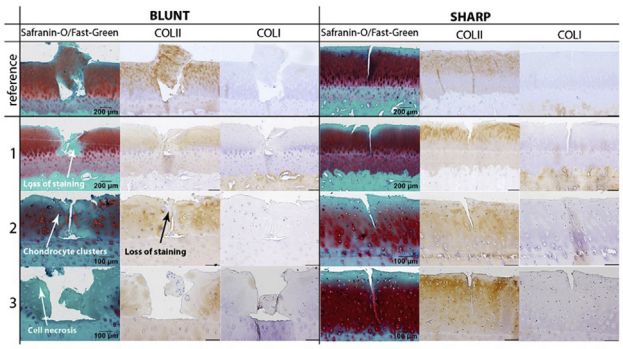

Fig1 *Typical histological sections of articular cartilage surfaces with blunt and sharp grooves. Reference shows a freshly made blunt and sharp lesion in a cadaver joint.*

were grooved via arthrotomy. Blunt and sharp grooves were randomly assigned to either of the two joints. Blunt grooves were made using a hooked arthroscopic probe with a sharpened tip. Sharp grooves were made with a surgical blade that was clamped in a custom-made device. The contra-lateral joints were sham-operated. After 3 weeks of box rest, the ponies were trained for 8 weeks on a treadmill, followed by free exercise in a group shed or at pasture until the end of the study. Radiographs of both carpal joints, taken at baseline and 38 weeks, were scored for osteoarthritic changes. After euthanasia at 39 weeks, osteochondral samples were harvested. Cartilage thickness was measured using micro-CT and biomechanical properties were measured by indentation testing. Histopathological OARSI scoring was performed on Safranin-O/Fast-green stained sections and collagen type-I and II staining was evaluated qualitatively.

Results: Grooved joints showed higher OARSI scores compared with the contra-lateral control joints ($p < 0.0001$) at 39 weeks. Blunt lesions were inherently larger and caused more tissue loss than sharp lesions. This resulted in a more extensive loss of proteoglycans and more pronounced cell cluster formation and focal cell loss in the adjacent cartilage (Fig1). Consequently, higher OARSI scores were observed in blunt-grooved than in sharp-grooved cartilage ($p = 0.007$). Cartilage thickness did not differ between grooved and control joints, but the cartilage stiffness trended lower in grooved joints. The lower stiffness was significant for the equilibrium modulus of sharp-grooved cartilage and the instantaneous modulus of blunt-grooved cartilage, in the radiocarpal joint. In the middle carpal joint, the 'kissing' site of blunt grooves displayed a significantly lower equilibrium modulus than cartilage in the control joint (Fig2). Radiographic scores of the carpal joints increased mildly but significantly in both grooved ($p = 0.0003$) and control ($p = 0.163$) joints, although the highest mean increase was observed in the blunt-grooved radiocarpal joint.

Conclusions: Both blunt and sharp articular cartilage grooves in the equine carpal joint were not spontaneously repaired and led to various degrees of degenerative changes within the surrounding tissue over a 39-week follow-up period. The tissue response was different for blunt and sharp injuries. These findings underline the importance of lesion morphology in combination with the loading profile in relation to tissue response to trauma and progression of damage. This is also important when considering or testing treatment strategies because biochemical composition, cell viability, structure, and mechanical properties of the lesion margin may affect the integration of cartilage repair tissue. Furthermore, this data could be highly valuable for the validation of computational models aiming at prediction of the progression of focal defects and development of post-traumatic OA.

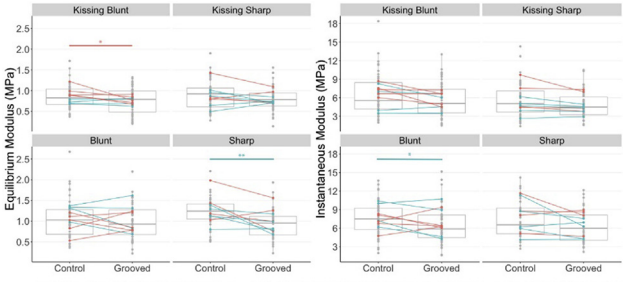

Fig2 *Cartilage biomechanical properties at the 39-week endpoint. Spaghetti plots show cartilage equilibrium modulus (A) and instantaneous modulus (B) averaged over 6 measured locations in the radiocarpal (green lines) and middle carpal (red lines) joints. Grey boxplots represent medians with interquartile ranges of all measured locations. * p <0.05; ** p <0.01.*

306
ELECTROACUPUNCTURE ALLEVIATES OSTEOARTHRITIS BY SUPPRESSING NLRP3 INFLAMMASOME ACTIVATION IN GUINEA PIGS

Z. Wang, P. Yuan, B. Dong, X. Li, B. Wang, H. Jia, W. Kang, D. Liu. *Shaanxi Univ. of Chinese Med., Xianyang, China*

Purpose: The aim of this study was to investigate whether Electroaucpuncture (EA) may alleviate osteoarthritis by suppressing NLRP3 inflammasome activation in guinea pigs.

Methods: Six-month-old male Hartley guinea pigs with spontaneous aging -related OA model were used in this study . Thermal hyperalgesia and mechanical allodynia was tested with the hot plate test and von Frey filaments. The expression of NLRP3 inflammsome and downstream proteins were quantified by using western blotting.

Results: Electroaucpuncture treatment significantly decreased the expression of NLRP3 inflammsome and the downstream protein expression of caspase-1, IL-1β.Electroaucpuncture significantly increased mechanical threshold, thermal latency in guinea pigs. Morover, electroaucpuncture also decreased the expression of MMP-13 and reduced the cartilage tissue damage.

Conclusions: EA can improve pain symptoms and cartilage tissue damage of OA models in guinea pigs,which may be related to its inhibition of the activation of NLRP3 inflammasome.

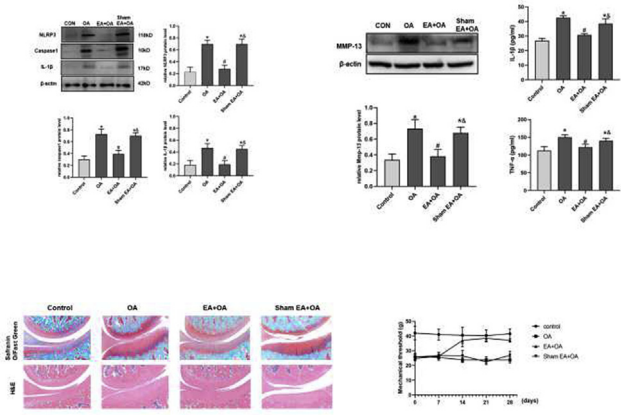

307
IDENTIFING THE GENDER-SPECIFIC GENES AND PATHWAYS IN OSTEOARTHRITIS BY BIOINFROMATICS

X. Wei, Z. Dong, L. Cheng, Z. Guo, Z. Lv. *The second Hosp. of Shanxi Med. Univ., Taiyuan, China*

Purpose: Female population shows higher OA incidence rates and severity compare to male in large joint. Except the effects of hormone, the underlying mechanisms are still largely unknown. The purpose of this study was to identify the key genes and pathways in gender differences of OA, and to explore the potential mechanisms.

Methods: Three different Series (GSE12021, GSE55475 and GSE55584) were obtained from the Gene Expression Omnibus (GEO) database. The raw data were integrated and divided into four groups (female OA, female normal, male OA and male normal group) before we screened the differently expressed genes (DEGs) using R programing language. The Venn diagrams were used to visualize the relationships of up and down regulated genes. The Gene Ontology functional and KEGG pathway enrichment of DEGs were analyzed using DAVID online analyses. We also created the protein-protein interaction networks of the DEGs. Final hub genes for both genders were identified respectively using nine different topological methods through CytoHubba. And some of the important final hub genes were validated by RT-qPCR.